

Driven large contact angle droplets on chemically heterogeneous substrates

D. HERDE¹, U. THIELE², S. HERMINGHAUS¹ and M. BRINKMANN^{1,3}

¹ Max Planck Institute for Dynamics and Self-Organization - 37077 Göttingen, Germany, EU

² Department of Mathematical Sciences, Loughborough University - Loughborough LE11 3TU, UK, EU

³ Experimental Physics, Saarland University - 66123 Saarbrücken, Germany, EU

received 27 June 2012; accepted in final form 10 September 2012

published online 16 October 2012

PACS 68.08.Bc – Liquid-solid interfaces: Wetting

PACS 47.55.D- – Drops and bubbles

PACS 47.20.Ky – Nonlinearity, bifurcation and symmetry breaking

Abstract – We study the depinning and subsequent motion of two-dimensional droplets with large contact angles that are driven by a body force on flat substrates decorated with a sinusoidal wettability pattern. To this end, we solve the Stokes equation employing a boundary element method. At the substrate a Navier slip condition and a spatially varying microscopic contact angle are imposed. Depending on the substrate properties, we observe a range of driving forces where resting and periodically moving droplets are found, even though inertial effects are neglected. This is possible in the considered overdamped regime because additional energy is stored in the non-equilibrium configuration of the droplet interfaces. Finally, we present the dependence of the driving at de- and repinning on wettability contrast and slip length, complemented by a bifurcation analysis of pinned-droplet configurations.

Copyright © EPLA, 2012

Introduction. – The dynamics of partially wetting droplets on heterogeneous substrates is relevant not only from the perspective of fundamental research [1] as it has direct applications in coating technology [2], microfluidics [3], and enhanced oil recovery [4]. Microscopic roughness and heterogeneities of the surface composition are the main cause for contact line pinning which leads to contact angle hysteresis and a low overall droplet mobility. Here we present a numerical study of droplet depinning for large contact angle droplets to elucidate the interplay between wettability contrast, the length scale of the substrate heterogeneities, and the slip length. For simplicity, we consider two-dimensional droplets which allow us to construct the energy landscape of a droplet and to track local energy minima during changes of the control parameter. To study the droplet moving over the heterogeneous substrate after depinning, we consider the droplet dynamics in the limit of high viscosity, *i.e.*, small Reynolds numbers. The evolution of the free-surface shape and position of the droplet is obtained by numerically solving the Stokes equations using the boundary element method (BEM). Interestingly, we observe a bistability of periodic motion and droplet pinning even though inertia, one of the primary arguments for bistable behaviour in tribology [5], is neglected in the Stokes limit.

Most studies of contact line dynamics that employ continuum models regard chemically homogeneous and flat substrates [1,6]. Effects of regular arrays of heterogeneities have recently been taken into account in studies of wettability-driven droplet spreading [7] and of droplet depinning under the influence of a lateral driving force [8,9]. Spreading on random topographical substrates has also been studied extensively [10,11]. These studies employ a long-wave evolution equation for the drop profile [12] that restricts them to droplets with small contact angles and small wettability contrasts (or shallow corrugations). Therefore, it is, for instance, not known which of the depinning transitions described in refs. [8,9] occur for droplets with large contact angles. Other methods employed to study the motion of liquid fronts or droplets over heterogeneous substrates include Lattice Boltzmann [13], phase field [14], and molecular-dynamics [15] simulations.

Here, we study droplets of arbitrarily large contact angles and consider their depinning transitions and subsequent droplet mobility on substrates with a chemical heterogeneity corresponding to a periodic wettability pattern. In contrast to [9] where the droplets are small compared to the distance of the defects, we focus on characteristic length scales for the heterogeneities well below the droplet size. The droplet is immersed in an

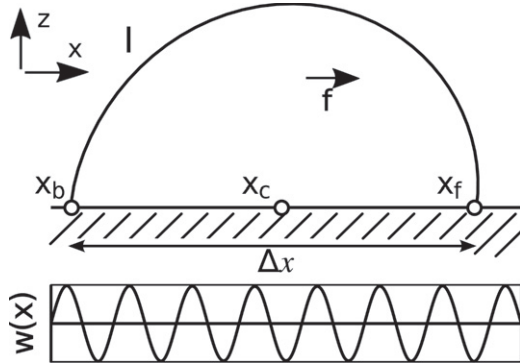


Fig. 1: Two-dimensional, large contact angle droplet with base length Δx centered around x_c sitting on a flat substrate with a sinusoidally varying wetting energy $w(x)$. The droplet is driven by a body force f parallel to the substrate.

inviscid fluid and driven by a constant body force parallel to the substrate. In this system we study the critical driving force where the droplet de- and repins, and the droplet mobility as a function of the wetting properties of the substrate and the slip length.

Static model. – The critical body force needed to mobilise a static droplet is studied using two methods. The first one is based on the observation that the energy landscape of a static two-dimensional droplet only depends on two coordinates, the positions of the front and back contact point. Interfacial instabilities and depinning can be detected by following the set of extremal points in the energy landscape as control parameters are changed. The second method considers the set of solutions to the ordinary differential equation which governs the equilibrium shape of the droplets. In this approach, static configurations of the free interface are followed in the space of control parameters using numerical continuation [16].

Energy landscapes. The total energy of the droplet on a vertical substrate, as visualised in fig. 1, is the sum of interfacial and gravitational energy, and reads

$$E\{\mathcal{S}\} = \gamma\ell + gA x_o + \int_{x_b}^{x_f} dx w(x), \quad (1)$$

where γ is the energy of the free surface per length and ℓ is the corresponding arclength. The second term on the RHS of eq. (1) accounts for the gravitational energy of the droplet with cross-sectional area A and lateral center-of-mass position x_o . The magnitude of the external driving is controlled by the body force per area, g . We use the total driving $f = gA$ as control parameter. The third term on the RHS accounts for wettability in terms of the position-dependent surface energy $w(x)$. It corresponds to the difference between the solid/liquid and solid/vapor surface energies per unit length normalised with γ . Now we consider dimensionless rescaled quantities by setting the interfacial energy, γ , and the cross-sectional area, A , equal to unity.

Mechanically stable two-dimensional droplets correspond to local minima of the constrained droplet energy

$$E_r(x_f, x_b) = \min_{\mathcal{S} \in C(x_f, x_b)} (E\{\mathcal{S}\}), \quad (2)$$

i.e., to minima of the total energy equation (1), over the subset \mathcal{C} of interfacial shapes \mathcal{S} with the front and back contact line at positions x_f and x_b , respectively, and with a cross-sectional area $A=1$. As sketched in fig. 1, instead of the positions of the contact lines one may equivalently consider the droplet's base length $\Delta x = x_f - x_b$ and lateral position $x_c = (x_f + x_b)/2$ of the midpoint of the wet section of the substrate. To determine $E_r(\Delta x, x_c)$ we use the free software package *Surface Evolver* [17].

We assume a periodic surface energy of the form

$$w(x) = w_o + \Delta w \cos(2\pi k x/L_o), \quad (3)$$

where L_o is the base length of a droplet with unit area on a homogeneous substrate with wetting energy w_o . The periodicity k represents the number of substrate modulations covered by a droplet. The maximal wettability contrast is $2\Delta w$.

Integration of eq. (3) from x_b to x_f together with the gravitational energy leads to a position-dependent contribution

$$E_p = f x_o + w_o \Delta x + \frac{\Delta w L_o}{2\pi k} \sin(2\pi k x/L_o)|_{x_c-\Delta x/2}^{x_c+\Delta x/2} \quad (4)$$

to the total droplet energy. The explicit form of the function $E_p(\Delta x, x_c)$ and the numerically determined function $E_c(\Delta x)$ that gives the energy of the free interface for a given baselength allow us to determine the set of extrema of the energy landscape of the constrained droplet energy $E_r(\Delta x, x_c)$.

Without wetting contrast $\Delta w = 0$ and at zero driving $f = 0$, the function $E_r(\Delta x, x_c)$ displays a single straight valley into the direction of x_c at the preferred base length Δx which is determined by the wetting energy w_o . For $\Delta w \neq 0$ a periodic modulation of $E_r(\Delta x, x_c)$ in the direction of x_c appears. Together with the linear gravitational contribution, $E_r(\Delta x, x_c)$ displays a periodic landscape of local maxima, minima, and saddle points.

Changes in the control parameters f , Δw , or w_o lead to changes in the tracked position and number of extrema found for each period of the wettability pattern. Monitoring the contact angles θ_f and θ_b at the front and back contact point of the droplet, respectively, shows that, as expected, droplets corresponding to an extremum of $E_r(\Delta x, x_c)$ satisfy the Young-Dupré equation

$$\cos \theta_i = w(x_i) \quad \text{for } i \in \{f, b\} \quad (5)$$

within numerical tolerances.

For the simple wettability pattern chosen, the number of local minima at fixed period is monotonically decreasing as the driving f is increased. Hence, we can define complete depinning of the droplet from the heterogeneities as the

parameter value f^\uparrow where the last local minimum of the energy landscape disappears. In other words, for driving forces above f^\uparrow no mechanically stable steady droplets exist.

Shape equation. Another possibility to obtain the spectrum of steady droplets pinned to the heterogeneities of the surface energies is to satisfy the conditions of mechanical equilibrium for the interface and at the contact points. The shape of the droplet can be given by a parametric curve $(x(u), y(u))$ with a parameter $u \in [0, 1]$. The local curvature $\kappa(u)$ of the interface, with u as control variable of the parametrised curve describing the free interface, has to balance the pressure difference according to the Laplace equation

$$\kappa(u) = f x(u) + \lambda \quad (6)$$

which governs the shape of a droplet under the action of a body force density f . Here λ is the Laplace pressure that has to be chosen to satisfy the constraint of a fixed enclosed area $A = 1$.

Provided the interface does not exhibit overhangs, its curvature κ can be expressed in Monge parameterization $y(x)$ as

$$\kappa(x) = -\frac{y''}{(1+y'^2)^{\frac{3}{2}}}, \quad (7)$$

where primes denote derivatives with respect to x . The slope of the interface at the contact line has to satisfy the boundary conditions

$$\tan \theta(x_i) = y'(x_i) \quad \text{for } i \in \{b, f\} \quad (8)$$

according to the local contact angle $\theta(x)$ given by Young's equation (5) and the surface energy (3).

Here we use the continuation algorithms bundled in the free software package *Auto07p* [16] to solve the ordinary differential equation (6) and boundary condition (8) starting from the known spherical cap solution on a homogeneous substrate. Such methods are extensively used in the context of long-wave models [8,18].

Note that in the explicit construction of mechanical equilibria, each of them must correspond to a minimum, maximum or saddle point of the energy landscape $E_r(\Delta x, x_c)$ discussed previously. However, the stability of the extrema is *a priori* not known and has to be obtained via a combination of energy measurements and a discussion of the obtained bifurcational structure.

Dynamic model. – For sufficiently small droplets inertial effects are negligible and the droplet evolution may be studied in the limit of completely overdamped fluid dynamics, *i.e.*, by solving the Stokes equations for a droplet of incompressible viscous liquid immersed in an inviscid fluid of zero density [19]. We chose our time scale such that the dynamic viscosity of the liquid equals unity. At the free interface of the droplet we impose a vanishing tangential force while the normal force is (for

$\gamma=1$) given by the local curvature of the free interface, κ , together with the gravitational contribution. The boundary condition at the flat substrate is the Navier slip condition $\partial_z v_x = v_x/l_s$, relating the value of the tangential velocity component v_x to its derivative perpendicular to the substrate. The linear interpolation length l_s is the slip length. We solve the Stokes equation together with the boundary conditions at the free interface and substrate using the boundary element method (BEM) [19] employing a piecewise linear discretised boundary of the droplet with increased refinement in the contact point regions.

For a given droplet configuration, we first determine the curvature of the free interface and, hence, the Laplace pressure at the interface. In a next step we obtain the velocity of the free interface from the solution of the BEM equation. This velocity field is used to evolve the shape of the free interface. On the two boundary elements where the free interface is in contact with the substrate, we enforce the local position-dependent microscopic contact angle. A similar method is used in refs. [20,21] to model moving droplets. We used a sufficiently high discretisation such that the numerical slip becomes negligible compared to the physical slip included in the model.

Results and discussion. – Before addressing moving droplets on a substrate with a wettability pattern it is instructive to consider the spectrum of possible steady states. On microscopically heterogeneous substrates, a set of steady droplets with different macroscopic contact angles can be observed experimentally. Following the lines of the work of Vellingiri *et al.* [22] for the case without gravity, we study the existence and stability of such solutions depending on wetting energy contrast Δw , wettability periodicity k and driving force f . Varying k in eq. (3) we find by numerical continuation a number of solution branches to the shape equation, eq. (6), for $f=0$ as displayed in fig. 2(a). Inspection of the droplet shapes on these branches reveals three different types of equilibria, as shown in fig. 2(b), which depicts the energy landscape for $k=5$: Instead of a single, translationally invariant minimum of the restricted energy $E_r(\Delta x, x_c)$, as observed for a homogeneous substrate, we find a corrugated energy landscape with a number of minima, maxima, and saddle points.

The first and second type of equilibria correspond to droplets that are located symmetrically with respect to the minima (on vertical lines in fig. 2(b)) and maxima (at $x_c=0$ in fig. 2(b)) of the sinusoidal wetting energy pattern $w(x)$, respectively. Both types may be either stable or unstable as indicated by solid and dashed lines in fig. 2(a), respectively. The third type are the saddle points of the energy landscape that always correspond to unstable droplets. They sit in an asymmetric way on the wettability pattern $w(x)$ (dotted lines in fig. 2(a) and crosses in fig. 2(b)), and have base lengths Δx that are a multiple of the period $L=L_o/k$.

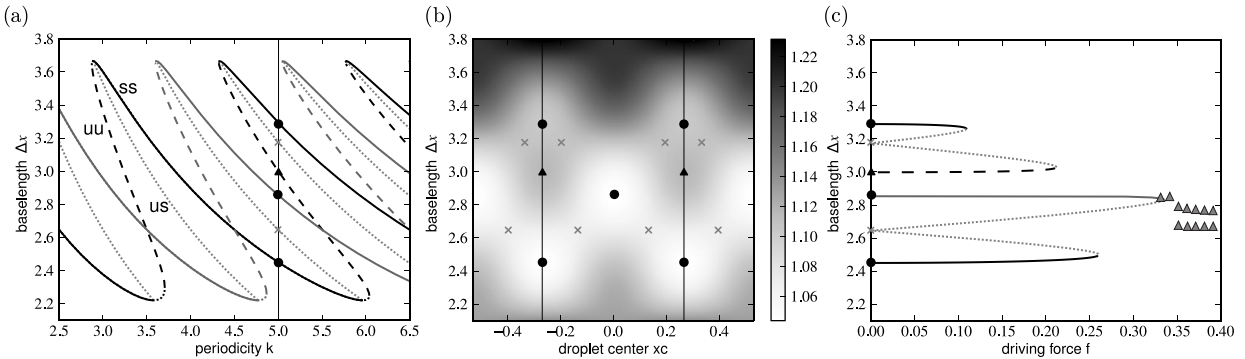


Fig. 2: (a) Base length Δx of extremal droplet configurations as a function of the periodicity k for vanishing body force $f = 0$. Solid lines represent stable droplets (ss) while dotted and dashed lines represent unstable droplets with one (us) or two (uu) unstable directions, respectively. At $k = 5$, local maxima, minima, and saddle points are marked by triangle, circle and cross symbols, respectively. (b) Density plot of the restricted droplet energy $E_r(\Delta x, x_c)$ at $f = 0$ and $k = 5$ showing the displacement of the marked solutions on the substrate and the degeneration of the saddle points with vertical lines delimiting one period of the substrate. (c) Bifurcation diagram for increasing driving force $f > 0$ for $k = 5$ showing the steady droplets (lines) and the minimal and maximal base length of periodically moving droplets (triangles). For plots (a) to (c), the sinusoidally varying wetting energy has an amplitude $\Delta w = 0.2$, mean $w_o = -0.707$ (corresponding to a contact angle $\theta = 45^\circ$) and slip length $l_s = 10$.

The (double) branches of asymmetric solutions connect the two different branches of symmetric solutions via symmetry breaking pitchfork bifurcations and form thereby a similar snake and ladders bifurcation diagram as well known for localised states [23]. Here, the bifurcations occur at points where the base length Δx as a function of k of the first and second type of droplets displays either a minimum or a maximum (fig. 2(a)). In terms of equilibria of the energy $E_r(\Delta x, x_c)$, a local minimum and a pair of saddle points corresponding to asymmetric solutions merge into a single saddle point that corresponds to a symmetric solution. Droplet shapes corresponding to the local minimum and the single saddle point exhibit the same symmetry, *i.e.*, reflection symmetry with respect to either a minimum or a maximum of $w(x)$. Following the symmetric branches beyond this bifurcation point to the turning point, the saddle point transforms into a local maximum.

The number of mechanically stable droplet equilibria increases as the periodicity of the pattern is reduced while the upper and lower limit for Δx are fixed by the minimal and maximal wetting energy. These relations can easily be derived from the observation that any equilibrium shape of the free interface must be a circular arc matching the local contact angles according to the equation of Young-Dupré (5). This has already been described in ref. [7] where the spreading of two-dimensional droplets under the action of interfacial forces is investigated.

To understand the depinning of droplets from the wettability pattern we follow the steady-solution branches of eqs. (6) and (8) when the body force f is increased at fixed periodicity k , average wettability w_o , and wetting contrast Δw . In fig. 2(c) the resulting droplet base lengths Δx are shown as a function of f for the case of $k = 5$. A body force $f > 0$ amounts to an overall tilt of the energy

landscape in fig. 2 into positive x_c -direction and a change of the energy contribution E_c fixed by the contour of the free interface.

Since the body force breaks the reflection symmetry of the wettability pattern a classification of equilibrium droplets according to discrete symmetries can no longer be applied. However, the spectrum of solutions evolves for $f > 0$ continuously from the one at $f = 0$ which displays these symmetries. Discontinuous changes of the number of solutions only occur whenever a saddle point and a local extremum of $E_r(\Delta x, x_c)$ merge and disappear in a saddle-node bifurcation (cf. also fig. 2(c)). For the sinusoidal wettability pattern, eq. (3), we observe that the number of steady solutions decreases as the external driving is increased. We note that the loss of a stable solution branch is correlated with the contact point at the droplet back or front reaching a maximum or minimum of the wettability, respectively.

To study the dynamics of depinned moving droplets we solve the Stokes equation as described above. A variety of different dynamical behaviours can be observed. For instance, as shown in fig. 3(a) small changes in the periodicity k can result in a transition from an anti-phase stick-slip motion where the velocities of the front and back contact points are phase-shifted by half a temporal period to an in-phase stick-slip motion, where front and back move synchronously.

The triangles in fig. 2(c) show the classical depinning scenario of a saddle-node infinite period (SNIPER) bifurcation. The branch of periodically moving droplets emerges at the saddle-node bifurcation with a period that diverges close to the critical point. This scenario is also observed for an overdamped mass point in a periodically modulated potential under constant driving where it is described by the Adler equation [8,24]. Figure 3(b) depicts

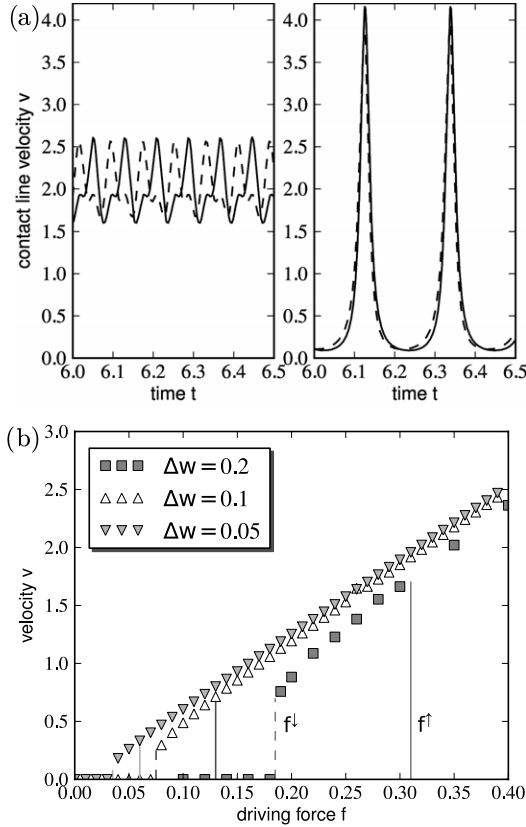


Fig. 3: (a) Velocity of the front (solid line) and back (dashed line) contact point over time showing (left) anti-phase motion at periodicity $k = 10$ and (right) in-phase motion at the slightly different $k = 10.25$ for $\Delta w = 0.2$, $f = 0.35$. (b) Final mean droplet velocity as a function of driving force f for heterogeneities Δw as given in the legend and $k = 10$, with the observed depinning (solid line) and repinning (dashed line) force. For (a) and (b) the average wetting energy is $w_o = 0$ ($\theta = 90^\circ$), and the slip length $l_s = 10$.

the resulting mean droplet velocity v as a function of the driving f for the case of a large slip length $l_s = 10$ and large average contact angle of 90° . The average velocity is monotonically decreasing with increasing Δw because the viscous dissipation resulting from the periodic droplet deformation increases, resulting in a higher effective friction.

If one starts with a steady droplet and increases the driving f , the droplet depins at f^\uparrow (respective solid vertical lines in fig. 3(b)) where it jumps to a finite mean velocity. However, decreasing f again, one observes that below f^\uparrow the solution follows a different branch until f^\downarrow where in our simulations the mean velocity drops discontinuously to zero. This hysteresis loop differs substantially from the depinning via a SNIPER bifurcation where f at de- and repinning is identical [8]. The hysteresis leads to a parameter range of bistability where both, the static droplet and a periodically moving droplet, exist for identical substrate properties and forcing.

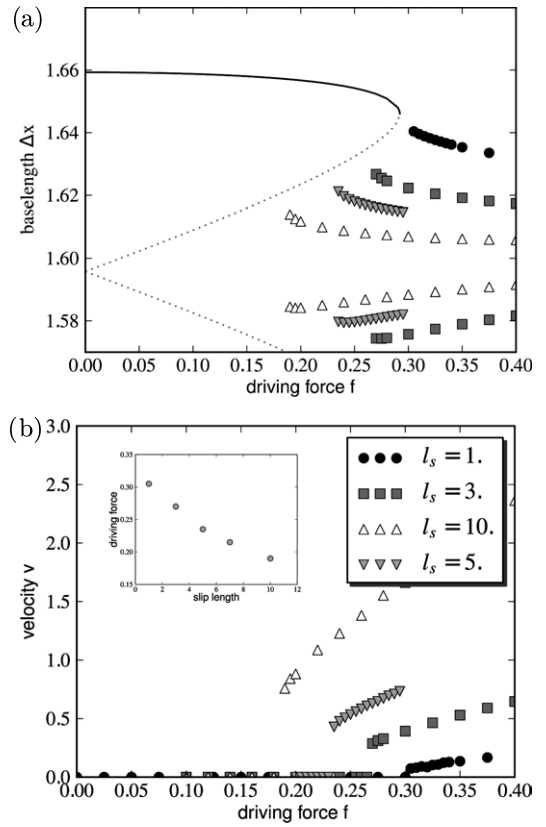


Fig. 4: (a) Minimal and maximal droplet base length Δx and (b) average droplet velocity v for static and periodically moving droplets as function of the driving force f for different slip length l_s as given in the legend of (b). The inset of (b) gives the minimal force f where moving droplets were observed as function of l_s . In all cases $w_o = 0$ ($\theta = 90^\circ$), $\Delta w = 0.2$, and $k = 10$.

To further analyse the repinning, fig. 4 shows how the hysteresis depends on the slip length: the minimum and maximum droplet base length Δx_{\max} and Δx_{\min} of periodically moving droplets together with the base lengths of the steady droplets are given for $w_o = 0$, $\Delta w = 0.2$, $k = 10$, and slip lengths from $l_s = 1$ to 10 . With decreasing slip length, the amplitude of the oscillations of Δx increases while the hysteresis range decreases. Such an observation of a hysteresis loop is commonly associated with inertial effects [5], however in the considered Stokes limit inertia is neglected.

Hysteresis in the present system is possible because the moving droplet is never at its equilibrium shape for the given positions of the back and front contact points. In the case of a large slip length the relaxation time scale of the interface can be larger than the time scale related to periodic deformations of the interface during motion. The excess in surface and wetting energy allows the droplet to pass the wettability barriers, analogous to the kinetic energy in a system with inertia.

Therefore, one may relate the droplet behaviour to two competing time scales: i) The scale of relaxation of the